SUBMITTED TO ApJ Letters
Preprint typeset using LaTeX style emulateapj v. 14/09/00

THE STELLAR VELOCITY DISPERSION OF THE LENS GALAXY IN MG2016+112 AT Z=1.004[1]

LÉON V.E. KOOPMANS
California Institute of Technology, TAPIR, 130-33, Pasadena, CA 91125
TOMMASO TREU
California Institute of Technology, Astronomy, 105-24, Pasadena, CA 91125
submitted to ApJ Letters

ABSTRACT

We present a direct measurement of the stellar velocity dispersion of the early-type lens galaxy D in the system MG2016+112 ($z = 1.004$), determined from a spectrum obtained with the *Echelle Spectrograph and Imager* (ESI) on the W.M. Keck–II Telescope, as part of the *Lenses Structure and Dynamics (LSD) Survey*. We find a velocity dispersion of $\sigma_{\rm ap} = 304 \pm 27$ km s^{-1} inside an effective circular aperture with a radius of $0.65''$, corresponding to a central velocity dispersion of $\sigma = 328 \pm 32$ km s^{-1}. From a *Hubble Space Telescope* F160W–band image, we measure the effective radius and effective surface brightness in order to determine the offset of the lens galaxy with respect to the local Fundamental Plane. The offset corresponds to an evolution of the rest-frame effective mass-to-light ratio of $\Delta \log(M/L_B) = -0.62 \pm 0.08$ from $z = 0$ to $z = 1.004$. By interpreting colors and offset of the FP with two independent stellar population synthesis models, we obtain a single-burst equivalent age of 2.8±0.8 Gyr (i.e. $z_{\rm f}$>1.9) and a supersolar metallicity of $\log[Z/Z_\odot]$=0.25±0.25. The lens galaxy is therefore a massive elliptical dominated by an old and metal rich stellar population at $z > 1$. The excellent agreement of the stellar velocity dispersion with that predicted from recent lens models confirms that the angular separation of the multiple images of the background QSO is predominantly due to the lens galaxy, and not to a massive "dark cluster", in agreement with recent weak lensing and X–ray observations. However, the significant overdensity of galaxies in the field might indicate that this system is a proto-cluster, in formation around galaxy D, responsible for the ∼10% external shear inferred from the strong lens models.

Subject headings: gravitational lensing — galaxies: elliptical and lenticular, cD — galaxies: evolution —- galaxies: formation — galaxies: structure

1. INTRODUCTION

In the cold dark matter (CDM) cosmological scenario, structures in the Universe form through hierarchical merging of smaller structures (White & Rees 1978; Blumenthal et al. 1984; Davis et al. 1985). Within this general framework, early-type galaxies (E/S0) in the cores of rich clusters form at high redshifts ($z > 2$), corresponding with the first dark-matter overdensity peaks, as opposed to a later formation epoch for field E/S0 (Kauffmann 1996). Clusters subsequently form around these seeds by accretion of smaller-mass galaxies, with significant structural and dynamical evolution occurring at more recent cosmological times. Recent observations have shown that massive cluster E/S0 were already assembled at $z > 1$ and subsequently evolved passively through ageing of their stellar populations (e.g. van Dokkum et al. 1998; Stanford, Eisenhardt & Dickinson 1998). Similarly, field E/S0 galaxies seem not to evolve dramatically between $z = 1$ and $z = 0$, both in number (Schade et al. 1999, Im et al. 2002) and structural properties (van Dokkum et al. 2001; Treu et al. 1999, 2001b, hereafter T01b), although secondary episodes of star formation might be frequent at $z < 1$ (Menanteau et al. 2001; Treu et al. 2002, hereafter T02). However, most observational results on the evolution of E/S0 concern the evolution of their stellar populations and little is known about the evolution of their internal structure.

To comprehensively quantify the luminosity, color *and* structural evolution of the stellar mass and of the dark-matter halo of E/S0 as function of redshift, we are conducting an observational program with the Echelle Spectrograph and Imager (ESI) on the W.M. Keck–II Telescope: the *Lenses Structure and Dynamics (LSD) Survey*. Aim of the *LSD survey* is to measure the internal kinematics of a dozen gravitational-lens galaxies up to $z = 1$, allowing a powerful combination of dynamical and lensing constraints on their mass distribution. The LSD Survey[1], its main goals and observing strategy will be described in detail elsewhere (Treu & Koopmans 2002, in preparation).

Here we present the first result of the *LSD Survey*, a measurement of the stellar velocity dispersion of the lens galaxy in the system MG2016+112 at $z = 1.004$. A summary of relevant prior observations and a new lens model can be found in Koopmans et al. (2002) and references therein. The primary lens galaxy (D) in MG2016+112 is the highest spectroscopically-confirmed redshift lens galaxy known to date. The suggestion that this lens was embedded in a massive "dark cluster", based on ASCA X-Ray observations (Hattori et al. 1997), was recently shown to be incorrect by high-resolution Chandra observations, showing no evidence for hot X-ray gas (Chartas

[1] Based on observations collected at W. M. Keck Observatory, which is operated jointly by the California Institute of Technology and the University of California, and with the NASA/ESA Hubble Space Telescope, obtained at STScI, which is operated by AURA, under NASA contract NAS5-26555.

[1] see also http://www.its.caltech.edu/~koopmans/LSD or http://www.astro.caltech.edu/~tt/LSD

et al. 2001). On the other hand, deep optical studies that show an overdensity of at least six bright E/S0 with the same redshift as the lens galaxy (Benitez et al. 1999; Soucail et al. 2001; Clowe et al. 2001). The absence of a significant weak-lensing signal (Clowe et al. 2001) and the absence of X-ray emission, however, shows that these galaxies are not associated with a massive evolved cluster.

In the following, we assume for definiteness that the Hubble constant, the matter density, and the cosmological constant are $H_0 = 65\ \mathrm{km\,s^{-1}\,Mpc^{-1}}$, $\Omega_m = 0.3$, and $\Omega_\Lambda = 0.7$, respectively.

2. OBSERVATIONS

2.1. *Keck Spectroscopy*

We observed MG2016+112 using ESI on the W.M. Keck–II Telescope during four consecutive nights (23–26 July, 2001), with a total integration time of 8.5 hrs. The seeing was good (0.″6-0.″8) and three out of four nights were photometric. Between each exposure of 1800 s, we dithered along the slit to allow for a better removal of sky residuals in the red end of the spectrum. The slit (20″ in length) was positioned at a position angle of 13° in order to include galaxies D and E, and arc C′ (see Fig. 2).

The slit width of 1.″25 yields an instrumental resolution of $30\,\mathrm{km\,s^{-1}}$ which is adequate for measuring the stellar velocity dispersion and remove narrow sky emission lines. Data reduction was performed using a newly developed IRAF package[2], that combines the procedures described in Treu et al. (1999, 2001a) and Smith et al. (2001) for the treatment of echelle distortions and sky subtraction. Spectra of G–K giants observed at twilight with a 0.3″ slit width were used as stellar templates, after appropriate smoothing to match the instrumental resolution of the 1.25″ slit. The best fit was obtained for a G4-III stellar template, using the Gauss–Hermite pixel-fitting software on the spectral region around the G band (Fig. 1). This yielded a stellar velocity dispersion of $\sigma_{\rm ap} = 304 \pm 27\,\mathrm{km\,s^{-1}}$ inside an effective circular aperture with radius 0.″65. The scatter in the fits for the different stellar templates was used to estimate the uncertainties related to template mismatches (see T01a). The error on $\sigma_{\rm ap}$ therefore includes both the random error contributions and the systematic uncertainties due to template mismatches, continuum fitting, and fitted spectral range. The inferred central velocity dispersion is $\sigma = (1.08 \pm 0.05) \cdot \sigma_{\rm ap}$, i. e. $\sigma = 328 \pm 32\ \mathrm{km\,s^{-1}}$. The correction is based on the average ratio (and spread) between the central stellar velocity dispersion (i.e. measured in a $R_e/8$ aperture) and the dispersion measured from a larger aperture ($\sim 2R_e$ in our case), as determined from local E/S0 (see T01a for details). The predicted velocity dispersion from isothermal gravitational-lens models, i.e. 320–340 km s^{-1} (Koopmans et al. 2002), is in excellent agreement with the spectroscopic determination of the central stellar velocity dispersion (see also Kochanek 1993, 1994 and Kochanek et al. 2000 for a general discussion). In addition, we detect [OII] emission from galaxies D and E at nearly identical redshifts ($z = 1.004$; Fig.2).

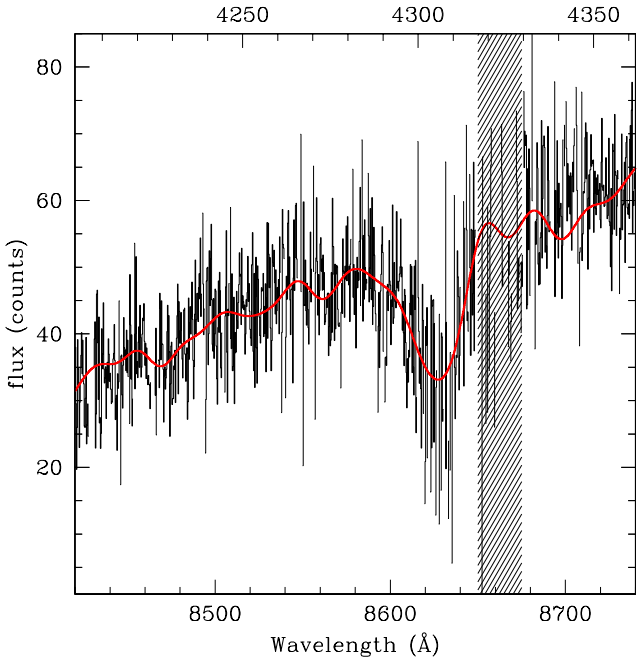

FIG. 1.— The G-band absorption feature at ∼4304 Å in the spectrum of galaxy D in MG2016+112. The rest-frame wavelength scale is shown on the top axis for reference. The smooth solid line is the best-fitting template (spectral-type G4–III) convolved to the measured velocity dispersion $\sigma_{\rm ap} = 304 \pm 27\ \mathrm{km\,s^{-1}}$. The dashed region is affected by sky-subtraction residuals and was omitted in the fit.

2.2. *Hubble Space Telescope Imaging*

Optical and infrared Hubble Space Telescope (HST) images of the system are available from the HST archive[3]. The Near Infrared Camera and Multi Object Spectrograph (NICMOS) Camera 2 imaged the galaxy in F160W for 5112s, while the Wide Field and Planetary Camera 2 imaged the system through filters F555W and F814W for 5200s each (Fig 2). The images were reduced and surface photometry performed on the F160W and F814W images as described in Treu et al. (1999, 2001a), except that cosmic rays rejection on the F814W image was performed using the LA Cosmic Algorithm (van Dokkum 2001). The lens galaxy is very faint at F555W and barely detected in the Planetary Camera images, yielding a very uncertain flux. The galaxy brightness profiles are well represented by an $R^{1/4}$ profile, but the F160W- and F814W–band effective radii are significantly different and the galaxy shows a significant reddening towards its core. We attribute the larger effective radius in F814W–band to a bluer extended envelope around galaxy D (seen as a "wing" in the brightness profile), which presumably comes from a younger stellar population that has been accreted from smaller galaxies (e.g. galaxy E). Because the F160W–band light is a better tracer of the underlying old stellar population (dominant in mass) and is not contaminated by the [OII] emission line (Fig.2), we only use $R_{e,F160W}$ for our analysis. In addition, the fits provided the integrated magnitudes and effective surface brightnesses. The relevant observational quantities of MG2016+112 are listed in Tab. 1. Rest frame photometric quantities are corrected for galactic extinction using E(B-V)=0.235 from Schlegel et al. (1998).

[2] EASI2D, developed by D. Sand and T. Treu; Sand et al. (2002), in prep.

[3] Obtained as part of the CASTLeS Survey

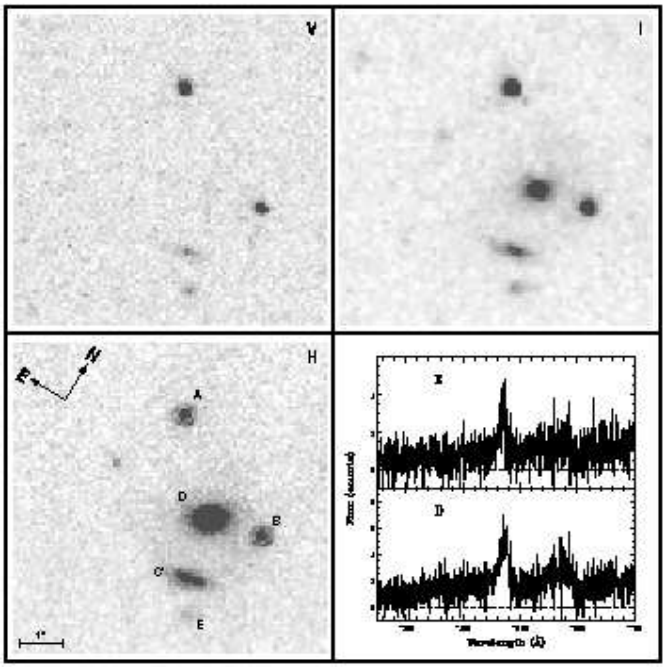

FIG. 2.— HST images of MG2016+112: WFPC2 F555W (V) and F814W (I) images, the NICMOS-2 F160W (H) image. The exposure times are 5200s (V and I), and 5120s (H), and the pixels scale are 0.0455″ (V), 0.1″ (I), 0.075″ (H). The two lensed quasar images (A and B), the primary lens galaxy (D), the arc C′ and the additional galaxy (E) are indicated on the H-band image. The emission from the [OII] doublet detected from galaxies E and D is shown in the bottom right panel. Note that the doublet in D is blended by the large velocity dispersion.

3. RESULTS

Using the stellar velocity dispersion, effective radius, effective surface brightness and colors of the lens galaxy, we can now quantify the evolution of its stellar mass-to-light ratio, as well as the age and metallicity of the dominant stellar population. A discussion is given in Sec. 4.

Recent studies have shown that E/S0 in clusters and in the field define a tight Fundamental Plane (FP) out to $z \sim 0.7 - 0.8$ (van Dokkum et al. 1998; T02), with slopes very similar to the ones observed in the local Universe. Assuming that galaxy D lies on a FP with slopes similar to those in the local Universe[4], we can obtain the evolution of the intercept γ of the FP with redshift, which is related to the evolution of the average effective mass to light ratio (M/L). In Fig. 3 we plot the evolution of the M/L for cluster and field E/S0 as function of redshift (small squares and pentagons; from T02), together with the value obtained for galaxy D (large filled square). From the local FP, one finds an offset $\Delta\mathrm{SB}_e = -1.55$ mag arcsec^2, which corresponds to $\Delta \log M/L_B = -0.62 \pm 0.08$ for pure luminosity evolution, the error being dominated by the observed FP parameters of galaxy D. We also note that errors on R_e and SB_e are correlated and partly cancel in the FP relation (e.g. Treu et al. 2001a; herafter T01a). The M/L evolution is intermediate between that of clusters and field E/S0, when we assume that a linear fit, $\Delta \log M/L_B \propto z$ (see Fig. 3), provides a good description of the data and can be extrapolated to $z = 1.004$. Eventhough this is only a single-galaxy measurement – not a determination of the FP at $z \sim 1$ – the inferred M/L evolution suggests that passive evolution of and old stellar population is a good representation of the evolution of massive E/S0 out to $z = 1.004$. Additional measurements, covering a range of FP parameters, are needed to confirm this result.

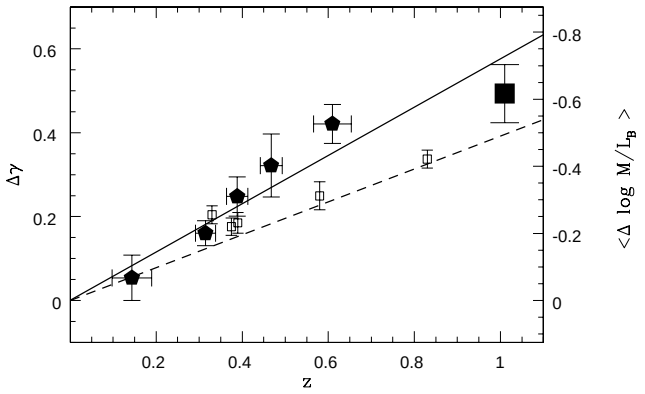

FIG. 3.— Evolution of the M/L as inferred from the evolution of the FP. Filled pentagons and open squares represent field and cluster measurements, respectively, while the thick full and dashed lines indicate linear fits to the M/L evolution for field and cluster E/S0 (see T02 for details). The large filled square at $z = 1.004$ indicates the M/L evolution of galaxy D in MG2016+112.

The color and M/L evolution of lens galaxy D can be used to infer age and metallicity of its stellar population. A single-burst stellar population, generated with two independent population synthesis codes (Bruzual & Charlot 1993; Fioc & Rocca-Volmerange 1997), gives a single-burst equivalent age of 2.8±0.8 Gyr (i.e. z_f>1.9) and a supersolar metallicity $\log[Z/Z_\odot]$=0.25±0.25 (Fig. 4), assuming there is no significant internal extinction in the lens galaxy. The contours in Fig. 4 are based on the χ^2 difference between the model and the observed color and mass-to-light ratio evolution (and their errors). Because the colors and the luminosity can be dominated by a small mass-fraction of bright young stars, this age should be regarded as a lower limit for age of the dominant stellar population. The supersolar metallicity is slightly higher, but within 1–σ consistent with results obtained from E/S0 in clusters at redshifts $z \approx 0.3 - 0.9$, which have been assembled through hierarchical merging of smaller galaxies (e.g. Ferreras, Charlot & Silk 1999).

4. DISCUSSION & CONCLUSIONS

We have presented a direct measurement of the stellar velocity dispersion of the lens galaxy in the highest spectroscopically-confirmed redshift lens system MG2016+112 ($z = 1.004$), as part of the *Lenses Structure and Dynamics (LSD) Survey*. The effective radius and surface brightness are determined from HST images, to compare the properties of the lens galaxy with those of E/S0 in the local Universe. The colors and evolution of $\mathrm{M/L}_B$ of its stellar population, as derived by comparison to the local FP, indicate an old (∼3 Gyr) metal-rich stellar population, consistent with a passively evolved single

[4] In the following, we adopt $\log R_e + \log h_{50} = 1.25 \log \sigma + 0.32\,\mathrm{SB}_e - 8.895$ (Bender et al. 1998) for the local FP in rest-frame B-band (see T01b for discussion). The uncertainties on the local determination of the FP are negligible in our analysis.

stellar population formed at $z_{\rm f} > 1.9$. The large stellar velocity dispersion and metallicity of the lens galaxy is comparable to the most massive present-day cluster galaxies (Ferreras et al. 1999; Fisher et al. 1995). In addition, the F814W-band surface brightness profile at large radii deviates slightly from the $R^{1/4}$ profile, possibly indicating an outer envelope, as typically found for brightest cluster galaxies and cD galaxies (Graham et al. 1996). This bluer envelope and the [OII] emission that we detect from galaxy D (see also Soucail et al. 2001) could be due to the accretion of a younger stellar populations from smaller gas-rich galaxies, such as the closest companion to galaxy D for which we detect [OII] in emission (Fig.2).

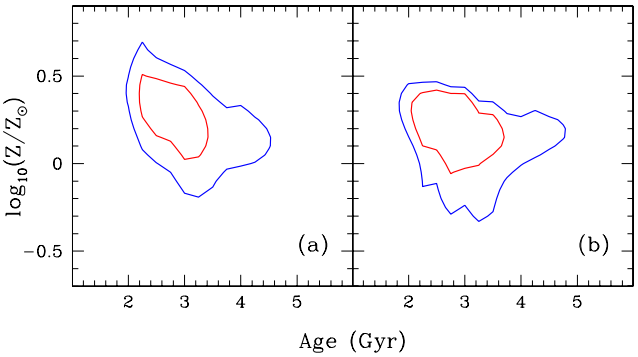

FIG. 4.— Likelihood contours of the age and metalicity of the stellar population of MG2016+112, galaxy D. The inner and outer contours indicate the 68% and 95% probability. Panels (a) and (b) are for population synthesis models from Bruzual & Charlot (1993) and Fioc & Rocca-Volmerange (1997), respectively.

This scenario is consistent with the gravitational-lens system being embedded in a galaxy overdensity (i.e. a proto-cluster; see also Benitez et al. 1999), which is not yet relaxed to a more centrally concentrated system and still shows evidence for ongoing merging and accretion. In addition, it would explain the absence of a significant weak-lensing signal (Clowe et al. 2001), the relatively small lensed-image separation, as well as constraints from recent Chandra X-ray observations (Chartas et al. 2001). In particular, the spread of the velocities of the galaxies in the overdensity (Soucail et al. 2001), if they are assumed to be virialized, implies a mass three times larger than the 3–σ upper limit inferred from the non-detection of extended X-ray emission with Chandra (Chartas et al. 2001). We therefore think that the assumption of virialization is *not* correct and that these galaxies form a (non-virialized) proto-cluster. Three galaxies in the field are spatially clustered at $z = 0.97$ and might be falling towards the overdensity with high velocity (Soucail et al. 2001), consistent with a cluster in formation.

Redshift (D)	1.004±0.001
$F160W$ (mag)	18.24±0.02
$F814W$–$F160W$ (mag)	3.3±0.1
$\mathrm{SB}_{e,F160W}$ (mag/arcsec^2)	17.64±0.40
$R_{e,F814W}$ (arcsec)	0.65±0.10
$R_{e,F160W}$ (arcsec)	0.31±0.06
$\sigma_*(< 0.65'')$ (km s^{-1})	304±27
b/a=$(1-e)$	0.75±0.10
Major axis P.A. (°)	121 ± 2
σ (km s^{-1})	328±32
$B-I$ (mag)	1.98±0.15
M_B (mag)	−22.53±0.10
M_I (mag)	−24.51±0.04
$\mathrm{SB}_{e,B}$ (mag/arcsec^2)	18.12±0.50
$\mathrm{SB}_{e,I}$ (mag/arcsec^2)	16.14±0.40

Table 1.— Observed spectro-photometric quantities of galaxy D in MG2016+112. The second part of the table lists rest-frame quantities, derived from the observed quantities (see text).

The use of the Gauss-Hermite Pixel Fitting Software developed by R. P. van der Marel and M. Franx is gratefully acknowledged. The ESI data were reduced using software developed in collaboration with D. Sand. We thank E. Agol, A. Benson, G. Bertin, R. Blandford, C. Conselice, R. Ellis, M. Stiavelli for comments on this manuscript. We acknowledge the use of the HST data collected by the CASTLES collaboration. LVEK and TT acknowledge support by grants from NSF and NASA (STSCI-AR-09222).

REFERENCES

Bender, R., Saglia, R. P., Ziegler, B., Belloni, P., Greggio, L., Hopp, U., & Bruzual, G. 1998, ApJ, 493, 529
Benitez N., Broadhurst T., Rosati P., Courbin F., Squires G., Lidman C., Magain P., 1999, ApJ, 527, 41
Blumenthal, G. R., Faber S. M., Primack J. R. & Rees, M. J., 1984, Nature, 311, 517
Bruzual A. G., Charlot S., 1993, ApJ, 405, 553
Chartas G., Bautz M., Garmire G., Jones C., Schneider D. P., 2001, ApJ, 550, L167
Clowe, D., N. Trentham, and J. Tonry 2001, A&A369, 16-25
Davis, M., Efstathiou, G., Frenk, C. S., White, S. D. M., 1985, ApJ, 292, 394
Ferreras, I., Charlot, S., Silk, J., 1999, ApJ, 521, 81
Fioc M., Rocca-Volmerange B., 1997, A&A, 326, 962
Fisher D., Illingworth G., Franx M., 1995, ApJ, 438, 562
Graham A., Lauer T. R., Colless M., Postman M., 1996, ApJ, 465
Hattori M. et al., 1997, Nature, 388, 148
Im, M., Faber, S. M., Koo, D. C., Phillips, A. C., Schiavon, R. P., Simard, L. & Willmer, C. N. A., 2002, ApJ, in press
Kauffmann, G., 1996, MNRAS, 281, 492
Kochanek, C. S., 1994, ApJ, 436, 66
Kochanek C. S. et al., 2000, ApJ, 543, 148
Koopmans L.V.E., Garrett M.A., Blandford R.D., Lawrence C.R., Patnaik A.R., Porcas R.W., 2002, MNRAS, accepted
Menanteau, F., Abraham, R. G., Ellis, R. S. 2001, MNRAS, 322, 1
Schade D. et al., 1999, ApJ, 525, 31
Schlegel D. J., Finkbeiner D. P., Davis M., 1998, ApJ, 500
Smith, G. P., Treu, T., Ellis, R. S., Smail, I. R., Kneib, J.-P., Frye, B. L., 2001, ApJ, 562, 635
Soucail G., Kneib J.-P., Jaunsen A. O., Hjorth J., Hattori M., Yamada T., 2001, A&A, 367, 747
Stanford, S. A., Eisenhardt, P. R., Dickinson M., 1998, ApJ, 492
Treu, T., Stiavelli, M., Casertano, S., Møller, P., Bertin, G., 2002, ApJ, 564, L13
Treu, T., Stiavelli, M., Casertano, S., Møller, P., Bertin, G., 1999, MNRAS, 308, 1037
Treu, T., Stiavelli, M., Møller, P., Casertano, S., & Bertin, G., 2001a, MNRAS, 326, 221
Treu, T., Stiavelli, M., Bertin, G., Casertano, S., Møller, P., 2001b, MNRAS, 326, 237
van Dokkum, P. G., 2001, PASP, 113, 1420
van Dokkum P. G., Franx M., Kelson D. D., Illingworth, G. D., 1998, ApJ, 504
van Dokkum P. G., Franx M., Fabricant D., Kelson D. D., Illingworth G. D., 1999, ApJ, 520, L98
van Dokkum, P. G., Stanford, S. A., Holden, B. P., Eisenhardt, P. R., Dickinson, M., & Elston, R., 2001, ApJ, 552, L104
White, S. D. M. & Rees, M. J., 1978, MNRAS, 183, 341